Cotten, G. R.; Sacks, W. *J. Polym. Sci., Part A* **1963**, *1*, 1345. (c) Feit, E. D., unpublished studies.
(26) (a) Cheng, H. N.; Schilling, F. C.; Bovey, F. A. *Macromolecules* **1976**, *9*, 363. (b) Bovey, F. A.; Schilling, F. C.; Cheng, H. N. In "Stabilization and Degradation of Polymers"; Allara, D. L., Hawkins, W.L., Eds.; American Chemical Society; Washington, DC, 1978; Adv. Chem. Ser. No. 169, p 133.
(27) Wu, T. K.; Ovenall, D. W.; Hoehn, H. H. In "Applications of Polymer Spectroscopy"; Brame, E. G., Ed.; Academic Press: New York, 1978; pp 19–40.
(28) Bennett, R. L.; Keller, A.; Stejny, J.; Murray, M. *J. Polym. Sci., Polym. Chem. Ed.* **1976**, *14*, 3027.
(29) Kuroki, T.; Sawaguchi, T.; Nikuni, S.; Ikemura, T. *J. Polym. Sci., Polym. Chem. Ed.* **1983**, *21*, 703.
(30) Bovey, F. A.; Schilling, F. C.; McCrackin, F. L.; Wagner, H. L. *Macromolecules* **1976**, *9*, 76.
(31) In this case, the number percent (NMR) and weight percent (activation analysis) are the same since CO and ethylene have nearly the same molecular weights.
(32) For a random model, % 1,4-dione = 100(% CO/% E)^2, where % CO and % E are the molar percents of CO and ethylene in the feed stock, respectively. Thus the % 1,4-diones structures expected in a 1.5% CO content is 0.023.[27]
(33) Correlation coefficients and confidence limits for IR and NMR data: carbonyl–Ar, 0.98 (99.9%); vinyl–Ar, 0.99 (99.9%); carbonyl–O_2, 1.00 (99.9%); vinyl–O_2, 0.91 (95%). Calculated following statistics programs of "Calculator Decision-Making Sourcebook"; Texas Instruments, 1977.
(34) Hartley, G. H.; Guillet, J. E. *Macromolecules* **1968**, *1*, 165.
(35) Dan, E.; Guillet, J. E. *Macromolecules* **1973**, *6*, 230.
(36) Guillet, J. E. *Naturwissenschaften* **1972**, *59*, 503.
(37) Schilling, F. C., unpublished studies.
(38) Hartley, G. H.; Guillet, J. E. *Macromolcules* **1968**, *1*, 413.
(39) Golemba, F. J.; Guillet, J. E. *Macromolecules* **1972**, *5*, 63.
(40) (a) Schultz, J. in "Polymer Materials Science"; Prentice-Hall: Englewood Cliffs, NJ, 1974; Chapter 2. (b) Wunderlich, B. in "Macromolecular Physics"; Academic Press: New York, 1973; Vol. 1, Chapter 3.
(41) Wagner, P. J. *Acc. Chem. Res.* **1971**, *4*, 168.
(42) Barltrop, J. A.; Coyle, J. D. In "Excited States in Organic Chemistry;" Wiley: New York, 1975, Chapter 7.
(43) Winkle, J. R.; Worsham, P. R.; Schanze, K. S.; Whitten, D. G. *J. Am. Chem. Soc.* **1983**, *105*, 3951.
(44) Slivinskas, J. A.; Guillet, J. E. *J. Polym. Sci., Polym. Chem. Ed.* **1973**, *11*, 3043.
(45) Dan, E.; Guillet, J. E. *Macromolecules* **1973**, *5*, 230.
(46) Wunderlich, B.; Poland, D. *J. Polym. Sci., Part A* **1963**, *1*, 357.
(47) As an alternative, consider chain packing in a trans–gauche conformation. Although γ-hydrogen transfer may be favored due to close proximity of the reaction centers, scission would be retarded due to restricted rotation. See ref 42 for examples of rotationally restricted ketones.
(48) Kamiya, Y.; Niki, E. In "Aspects of Degradation and Stabilization of Polymers"; Jellinek, H. H. G.,Ed.; Elsevier: New York, 1978; pp 80–147.
(49) Winslow, F. H.; Hellman, M. Y.; Matreyek, W.; Stills, S. M. *Polym. Eng. Sci.* **1966**, 273.
(50) Winslow, F. H.; Aloisio, C. J.; Hawkins, W. L.; Matreyek, W.; Matsuoka, S. *Chem. Ind.* **1963**, 533.
(51) Li, S. K. L.; Guillet, J. E. *Macromolecules* **1984**, *17*, 41.
(52) Wismontski-Knittel, T.; Kilp, T. *J. Polym. Sci., Polym. Chem. Ed.*, **1983**, *21*, 3209.

Backbone Dynamics of Poly(isopropyl acrylate) in Chloroform. A Deuterium NMR Study

Frank D. Blum,* Bojayan Durairaj, and Alapat S. Padmanabhan

Department of Chemistry, Drexel University, Philadelphia, Pennsylvania 19104.
Received November 30, 1983

ABSTRACT: The backbone dynamics of poly(isopropyl acrylate) (PIPA) in chloroform have been studied over a wide composition and temperature range using deuterium NMR. The polymer was specifically labeled with deuterium in the methine position so that only one resonance would be seen. The results of T_1 and T_2 measurements were used to test the log χ^2, VJGM, Bendler–Yaris (BY), and Skolnick–Yaris (SY) models of polymer reorientation. It was found that, even though all the models could mimic the data, they did not always fit the data in a physically realistic way. The log χ^2 model yielded results which were not physically realistic even in dilute solution. The results from the VJGM, BY, and SY models were roughly indistinguishable despite their different formulations. All three models contain two parameters, each of which are dominated by either fast or slow motions. Further, it was seen that in dilute solution, the fast motion has an energy of activation of about 5 kcal/mol which is independent of concentration. In more concentrated solutions the energies of activation for the slow-motion parameters are concentration dependent and range from 12 to 30 kcal/mol. In concentrated solutions, it was found that T_1 and T_2 cannot be represented by a single model but the T_2 measurements can be used to define a division between semidilute and concentrated solution when $[\eta]C_c \cong 30$ for PIPA–$CHCl_3$. It was also found that the T_2 values for the concentrated solutions could be fit by using a free volume approach. The free volume parameters were calculated and judged to be reasonable when compared to the other systems.

Introduction

The dynamics of the backbone and side chain of polymer molecules in solution have been studied by a wide variety of techniques.[1] The results from techniques such as dielectric relaxation, fluorescence depolarization, ESR spin labeling, and NMR relaxation studies can be used to test proposed models of polymer motion. The results from all of these techniques suggest that the reorientation of polymer segments is not adequately described as simple isotropic reorientation. NMR is particularly versatile for the study of polymer motion because it can be used to probe different moieties in a repeating unit, provided that each has a "resolved" resonance. Studies of relaxation times from ^1H, ^{13}C, and ^2H (to a lesser extent) NMR in dilute polymer solutions have been reviewed by Heatley[2] within the framework of models existing at that time.

The study of polymer dynamics using NMR in concentrated solutions is more complicated than in dilute solutions. As polymer concentrations are increased, the line widths broaden to the point of severe overlap, which makes it difficult to assign spectral features to individual resonances. Thus, detailed dynamics studies become difficult to perform with ^1H, ^{13}C, or ^2H NMR at natural abundance. Therefore, most quantitative polymer dynamics studies are carried out at concentrations less than 30 wt %. In the limit of bulk polymer, some of these problems can be overcome through the use of specialized techniques such as magic angle spinning. However, these are not easily

0024-9297/84/2217-2837$01.50/0

applicable to polymer solutions for a variety of reasons.

One possible solution to the problem of overlapping resonances in polymer solutions is the use of specific deuterium labeling. If only one position on the repeating unit is labeled, then there will not be any noticeable overlap of resonances because the natural abundance of deuterium is so low. Specific deuterium labeling is also an advantage because a deuterium nucleus attached to a carbon atom is relaxed via the electric quadrupole interaction. In that case the principal electric field gradient is along the C–D bond vector axis. Hence the effect is always intramolecular (while the proton NMR case may involve intermolecular contributions) and the results can be directly related to the reorientation of the C–D bond vector. Since deuterium relaxation times in general tend to be shorter than those of ^{13}C, the ^2H experiment also realizes a significant time savings over ^{13}C when the polymers are significantly enriched with deuterium.

In this study we have probed the dynamics of specifically deuterated poly(isopropyl acrylate) in chloroform. The polymer was enriched at the methine position and its dynamics were probed by using ^2H NMR relaxation times (i.e., T_1 and T_2). The purpose of the study was twofold. First, we wanted to observe dynamics of the polymer over a wide range of concentration and temperature. Second, we compared our results with those predicted from current motional models. We were interested in finding the limits of applicability of the models previously applied to rather limited data sets. Those chosen for comparison were the log χ^2 model proposed by Schaefer,[3] the diamond lattice model proposed by Monnerie et al. (VJGM),[4] the Bendler–Yaris model (BY),[5] and the Skolnick–Yaris (SY) model.[6-9] The experimental results represent a very broad range of NMR concentration and temperature data which can be used to examine polymer dynamics from a variety of viewpoints.

Experimental Section

Acrylonitrile-*d* was prepared in a manner similar to that found in the literature.[10,11] Acrylonitrile (**1a**) (20 mL), D_2O (20 mL), hydroquinone (0.2 g), and calcium oxide (0.8 g) were refluxed for 6.5 h. Under these conditions the methine proton is exchangeable. The acrylonitrile-*d* (**1b**) layer was separated, dried with anhydrous sodium sulfate, and distilled. Isopropyl alcohol (13.0 g) and D_2O (3.6 g) were added to a solution of acrylonitrile-*d* (10.6 g), sulfuric acid (40 g), hydroquinone (0.4 g), and D_2O (5.0 g) at 145 °C. The resulting isopropyl acrylate-*d* (**1c**) was then washed with water and sodium bicarbonate several times, dried with anhydrous sodium sulfate, and distilled from P_2O_5. The monomer was estimated to contain a 90:10 mole ratio of D/H in the methine position by comparison of the relative ^{13}C NMR signal intensities of the methine and methyl carbons in the protonated and deuterated polymers.

The isopropyl acrylate-*d* (**1c**) (10 g) was polymerized under a nitrogen atmosphere in toluene (20 g) using an azobis(isobutyronitrile) (AIBN) initiator. The polymerization was run at 65 °C for 6 h. The polymer was precipitated with methanol and dried in a vacuum oven. The reaction scheme is as follows:

$$\underset{\mathbf{1}}{CH_2{=}CR'R^2} \rightarrow -[CH_2{-}\underset{\mathbf{2}}{CD(CO_2CH(CH_3)_2)}]_n-$$

1a, R′ = H; R² = CN
b, R′ = D; R² = CN
c, R′ = D; R² = $CO_2CH(CH_3)_2$

The viscosity-average molecular weight was measured in benzene to be 98000 (DP = 1000) using Mark–Houwink constants from the literature.[12] The intrinsic viscosity of the polymer was also measured in $CHCl_3$ from 10 to 50 °C using an Ubbelohde viscometer in a thermostated bath. To check the molecular weight dependence of the relaxation times, a second sample was prepared with a molecular weight of 50000. From the carbon-13 spectrum of PIPA-*d* it was found that the polymer was predominantly atactic. On the basis of the tetrad analysis of the backbone methylene, the fractions of the racemic and meso diads were calculated to be 0.55 and 0.45, respectively. The assignments were based on previous studies on PIPA.[13]

Solutions for NMR studies were prepared by adding chloroform directly to weighed polymer in a 5-mm NMR tube. The highest molecular weight polymer (98000) was used for all samples. The tubes were sealed and no attempt was made to remove dissolved oxygen because of the shortness of the relaxation times. Deuterium NMR spectra were taken on a JEOL FX-90Q instrument operating at 13.8 MHz for deuterons. The T_1 values were measured by inversion–recovery (180°–*t*–90°) and the T_2's by the CPMG method.[14] In all cases the decay curves could be characterized by a single-exponential relaxation time. A pulse delay of at least $5T_1$ was used to allow for the deuterons to achieve equilibrium magnetization after each data acquisition. The relaxation times were calculated from the signal heights using a weighted log linear least-squares fit. The experimental errors in the relaxation time measurements are estimated to be about 10%. The experimentally determined relaxation times were independent of sample rotation rate. The temperature was maintained with the JEOL temperature controller which passed heated or cooled gas into the thermostated sample area. The uncertainty in the temperatures is ±1 °C.

Theoretical Background

The nuclear magnetic relaxational behavior of a deuterium nucleus directly bonded to a carbon atom is dominated by the electric quadrupole interaction. Since the principal electric field gradient can be taken as being along the C–D bond vector and nearly axially symmetric (η = 0, asymmetry parameter), the T_1 and T_2 values are given by[2,15]

$$\frac{1}{T_1} = \frac{3\pi^2}{20}(e^2qQ/h)^2[J(\omega_0) + 4J(2\omega_0)] \quad (1)$$

and

$$\frac{1}{T_2} = \frac{3\pi^2}{40}(e^2qQ/h)^2[3J(0) + 5J(\omega_0) + 2J(2\omega_0)] \quad (2)$$

where e^2qQ/h is the quadrupole coupling constant, $J(\omega)$ is the spectral density at frequency ω, and ω_0 is the Larmor frequency.

The problem confronting the polymer dynamicist is the evaluation of the spectral density, which is the Fourier transform of the autocorrelation function $G(t)$ or

$$J(\omega) = \int_{-\infty}^{\infty} G(t)e^{i\omega t}\,dt \quad (3)$$

In this case the autocorrelation function represents the correlation of the C–D bond vector axis at times 0 and t.[15] It is clear that while simple exponentially decaying autocorrelation functions describe the reorientation of small molecules, they are inadequate in the description of the motional behavior of polymer molecules in solution.[2] It is therefore appropriate to examine the more successful models of polymer dynamics which may describe the reorientation of polymers in solution.

The most versatile and popular empirical distribution of correlation times is the log χ^2 distribution proposed by Schaefer.[3] This model uses a skewed logarithmic distribution of correlation times which yields

$$J(\omega) = \int_{-\infty}^{\infty} \frac{\tau_0 F(s)[b^s - 1]\,ds}{(b-1)(1 + \omega^2\tau_0^2[(b^s - 1)/(b-1)]^2)} \quad (4)$$

where

$$s = \log_b [1 + (b-1)\tau/\tau_0] \quad (4a)$$

and

$$F(s) = \frac{P}{\Gamma(P)}(Ps)^{P-1}\exp(-Ps) \quad (4b)$$

Here, Γ represents the gamma function and b, P (width parameters), and τ_0 (mean correlation time) are chosen to fit the data. It is generally agreed that b and P are not totally independent[2] and the model is essentially a pseudo-two-parameter model.

A more molecular approach was taken by the Monnerie et al. (VJGM) model.[4] The model is based on three- and four-bond jumps on a diamond lattice. The result in terms of the spectral density is

$$J(\omega) = \left[\frac{2T_0T_d(T_0 - T_d)}{(T_0 - T_d)^2 + \omega^2T_0^2T_d^2}\right] \times \left(\frac{T_0}{2T_d}\right)^{0.5}\left[\frac{(1 + \omega^2T_0^2)^{0.5} + 1}{1 + \omega^2T_0^2}\right]^{0.5} + \left(\frac{T_0}{2T_d}\right)^{0.5}\left(\frac{T_0T_d}{T_0 - T_d}\right)\left[\frac{(1 + \omega^2T_0^2)^{0.5} - 1}{1 + \omega^2T_0^2}\right]^{0.5} - 1 \quad (5)$$

where T_0 and T_d are fitted and related to the three- and four-bond jump rate w_3 and w_4 by

$$T_0 = K_D^2(3.16w_3 - 9.61w_4) \quad (5a)$$

$$T_d = 4.74w_4 \quad (5b)$$

K_D takes the value of ln 9 if both the trans (anti) and gauche conformations are equally probable.

The remaining two models to be explored are those of Bendler and Yaris[5] and Skolnick and Yaris.[6] The Bendler–Yaris (BY) model is a continuum version of the discrete model proposed by Jones and Stockmayer.[16] In this limit, the solution of the one-dimensional diffusion equation is a series of plane waves which yield

$$J(\omega) = \frac{2}{(\omega_B^{1/2} - \omega_A^{1/2})}\int_{\omega_A^{1/2}}^{\omega_B^{1/2}} \frac{k^2}{\omega^2 + k^4}\,dk \quad (6)$$

where ω_A and ω_B (fitted) are the low- and high-frequency cutoff given by

$$\omega_A = (2/5)k_A^2\nu_0 \quad (6a)$$

$$\omega_B = (2/5)k_B^2\nu_0 \quad (6b)$$

where ν_0 is the three-bond jump rate and k_A and k_B are the short- and long-wavelength cutoff wave vectors.

Finally, the recent model of Skolnick and Yaris[6-8] (SY) extended the BY approach by including complex or real damping terms which effectively replace the low-frequency cutoff. Since we confine ourselves to two-parametrer fits, we will only consider the case of "real" damping. For this case, the SY model predicts

$$J(\omega) = \delta^{-1}\left[\frac{c(\omega)}{4k(\omega)}\ln\frac{A(\omega)}{B(\omega)} + \frac{S(\omega)}{2k(\omega)}\tan^{-1}\left(\frac{2k(\omega)S(\omega)}{k^2(\omega) - 1}\right)\right] \quad (7)$$

where

$$A(\omega) = 1 - 2k(\omega)c(\omega) + k^2(\omega) \quad (7a)$$

$$B(\omega) = 1 + 2k(\omega)c(\omega) + k^2(\omega) \quad (7b)$$

$$k(\omega) = (\omega^2 + \beta^2)^{1/4}/\delta^2 \quad (7c)$$

$$c(\omega) = [0.5(1 - \beta/(\omega^2 + \beta^2)^{0.5})]^{0.5} \quad (7d)$$

and

$$s(\omega) = [0.5(1 + \beta/(\omega^2 + \beta^2)^{0.5})]^{0.5} \quad (7e)$$

In this case δ and β are fitted to the experimental data and are related to the bond jump rate and damping constant, respectively. More specifically

$$\delta = D\omega_c^2 \quad (7f)$$

$$\omega_c = (k_{max}^2 - \beta/D)^{0.5} \quad (7g)$$

where D is the jump probability, ω_c is the short-wavelength cutoff, and k_{max} is the maximum value of the wave vector corresponding to the short-wavelength cutoff. The short-wavelength cutoff was introduced to account for the fact that there is a smallest displaceable unit in the polymer backbone.

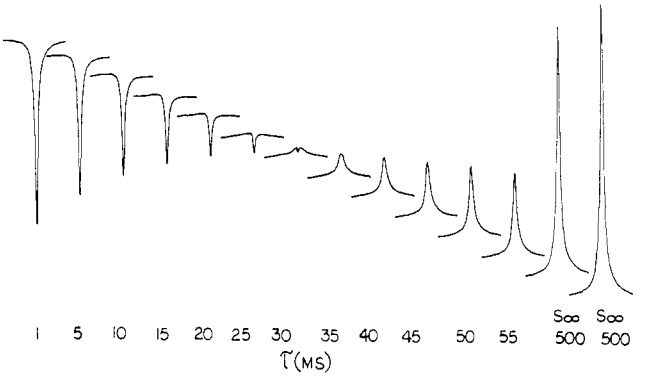

Figure 1. Typical deuterium inversion–recovery sequence for PIPA-*d*. Note the two resonances which can be seen near the null point (see text).

One might expect that the first three models proposed might adequately describe the reorientation of an isolated polymer chain. As the concentration is increased the limits of applicability of these models are not known. In contrast, the formulation of the SY model is such that we might expect the damping constant to be determined by the chain–chain interactions. Thus, it may be applicable to the results from concentrated solutions. In the following sections, we test the limits and/or validity of all four models using our deuterium NMR data.

Results

Shown in Figure 1 are the results of a typical inversion–recovery sequence for the deuterium nucleus on a 70.5 wt % PIPA-*d*–chloroform solution. The specifically labeled deuterium NMR technique has greater sensitivity than the natural-abundance carbon-13 methods. Only 50 transients were taken per delay value. As can be seen from the figure, the decay has the form of a single exponential, but a second superimposed resonance can be observed near the null point of the main resonance. Since both peaks have similar T_1 values, we conclude that both are from the same position on the polymer. A small difference in T_1 could be due to the differences in the mobilities of different triad species which would not be chemically shifted much in the deuterium spectra but could have slightly different relaxation times. It has been observed that there is a difference in the relaxation times for polymers of different tacticities as shown in studies on isotactic and syndiotactic PMMA in solution.[17] However, it appears that for atactic polymers, the relaxation times are roughly independent of the microstructure of the chains for several vinyl polymers.[18,19]

Shown in Figure 2A are the results of the T_1 measurements as a function of concentration and temperature. The results have also been tabulated in Table I. It can be seen that the plots for the low concentrations are similar to each other and show curvature at the low temperatures. At higher concentrations, T_1 minima are observed for concentrations greater than 70 wt % polymer. As the

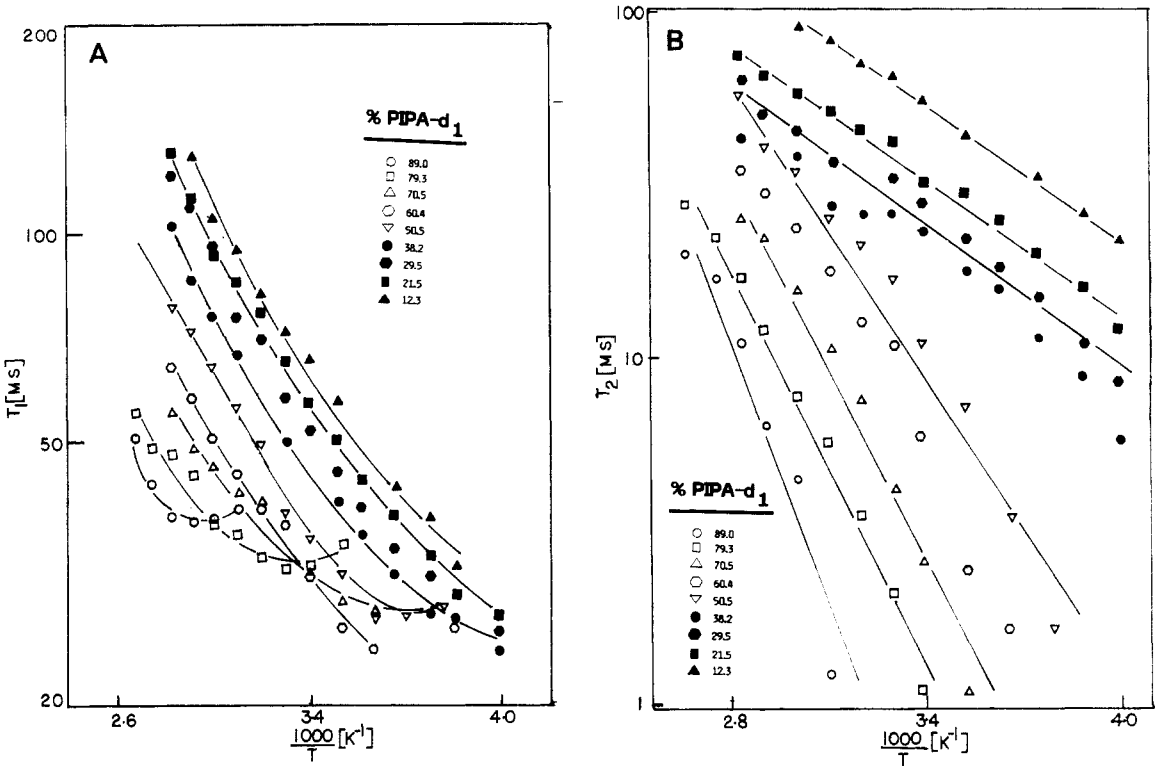

Figure 2. Deuterium relaxation time values as a function of concentration and temperature for (A) T_1 and (B) T_2. The lines are drawn to aid the eye only.

Table I
T_1 Values (ms) for the Different Concentrations of PIPA-*d* in $CHCl_3$ at Various Temperatures

	wt % PIPA								
T, °C	12.3	21.5	29.5	38.2	50.5	60.4	70.5	79.3	89.0
-34		28.3	26.7	24.8					
-24	33.3	29.6	27.4	27.6					
-20					29.8				
-16	39.0	34.0	32.0	28.3					
-10					28.9				
-7	43.3	39.2	35.7	31.6					
0					28.4	25.3			
3	44.0	40.8	37.3						
10	57.5	49.9	45.6	41.0	32.2	26.7	29.5		
20	65.9	56.7	51.6	39.8	36.4	31.7	32.6	33.0	
30	71.6	65.0	58.0	50.2	38.9	38.1	35.9	32.7	
40	82.4	77.5	70.1		49.5	39.8	39.9	33.8	
50	95.4	85.3	75.5	67.4	56.0	45.3	42.0	36.7	40.3
60	106	92.6	96.4	75.8	63.9	50.5	45.6	38.0	38.5
70	130	112	110	86.2	71.7	57.5	48.9	45.4	38.4
80		132	123	103	77.5	63.7	54.6	48.0	38.6
90								49.3	43.6
100								54.8	51.0

concentration is increased the minima shift to higher temperatures and higher T_1 values. The highest concentration reported is 89 wt % polymer.

In Figure 2B, and also in Table II, are shown the T_2 results as a function of temperature and concentration. The T_2 measurements made using the CPMG method were the same as those estimated from the line widths, for line widths greater than ca. 100 Hz. It was found that the line shapes were independent of the rate of sample rotation. As expected, the T_2's are a monotonic function of $1/T$. The decrease in T_2 with decreasing temperature becomes more pronounced for the more concentrated solutions. This is especially obvious for the T_2 values near temperatures corresponding to the T_1 minima seen in Figure 2A. Both T_1 and T_2 values were found to be independent of molecular weight for 50 wt % solutions for the 98 000 and 50 000 molecular weight samples. This is consistent with the earlier studies of PMMA.[17]

The data presented in Figure 2 represent a wide temperature–concentration range as well as a wide range of molecular mobility. In addition, the T_2 values provide a much more reliable, precise, second data set than the nuclear Overhauser enhancement (NOE) values which are usually used in ^{13}C studies of polymer dynamics. We will examine these data using the four different models summarized in the previous section. At this point we note that all four models examined can span our data set. However, we do not believe that the implications of these results are physically realistic. In the concentrated region where the models seem to fail we will use free volume concepts to model the T_2 data.

The results reported below for the various parameters were calculated from the T_1 and T_2 data assuming a quadrupole coupling constant for the backbone C–D of 165 kHz.[20,21] This value is typical of aliphatic carbon–deuteron bonds. The error introduced by the uncertainty in this

Table II
T_2 Values (ms) for the Different Concentrations of PIPA-*d* in $CHCl_3$ at Various Temperatures

	wt % PIPA								
T, °C	12.3	21.5	29.5	38.2	50.5	60.4	70.5	79.3	89.0
−34		9.23	6.01	3.92					
−24	21.6	11.9	8.47	5.81					
−20					0.83				
−16	26.0	16.1	10.9	8.80					
−10					1.92				
−7	33.6	20.0	14.9	11.7					
0					3.49	1.73			
3		25.0	18.2	15.9					
10	43.7	29.7	22.8	18.1	7.27	2.48	1.12		
20	54.9	32.3	27.5	23.4	11.3	6.05	2.62	1.18	0.212
30	65.6	42.4	33.0	26.5	17.2	10.9	4.25	2.06	0.398
40	69.8	45.7	35.0		20.7	12.5	7.53	3.53	0.663
50	83.4	51.1	36.0	27.2	25.0	18.0	10.4	5.77	1.25
60	88.6	56.2	44.7	37.9	34.5	24.0	16.0	7.72	4.50
70	112	64.9	50.0	45.1	39.4	30.5	22.2	12.1	6.38
80		75.5	63.0	52.4	54.0	37.2	29.8	16.8	11.5
90								22.3	17.3
100								28.2	25.2

Table III
Calculated Apparent Energies of Activation (kcal/mol) for Backbone Reorientation of PIPA-*d* from the Various Models Tested (See Text)

		VJGM		BY		SY	
wt. % PIPA	log χ^2	T_d	T_0	ω_B	ω_A	δ	β
12.3	2.4	4.3		2.4		6.6	
21.5	2.2	3.9		3.8		5.8	
29.5	3.2	4.1		3.9		6.2	
38.2	2.8	4.2		4.2		5.7	
50.5	2.7	5.7	12.3	5.2	12.2	6.0	10.8
60.4		5.1	13.8		13.5	5.4	13.1
70.5			17.4		15.7		18.5
79.3			17.9		15.4		17.0
89.0			24.0		22.8		29.0

value is not significant in its effect on the calculated motional parameters. Results for the log χ^2 (Figure 3), VJGM (Figure 4), and BY (Figure 5) models are shown in terms of the appropriate parameters. In many cases the behavior of the parameters is exponential with $1/T$. In such cases the calculated apparent energies of activation are shown in Table III.

The results of the data fitted with the log χ^2 model are shown in Figure 3. These data were fit using $b = 400$. In this range, variation of P and τ_0 could fit all of the data. As noted by Schaefer[3] the choice of b does not have a great effect on the calculated values of τ_0 which fit the data. Similar results are obtained for $b = 100$ and it appears that the qualitative features of Figure 3 are roughly independent of b. Values of P ranged from 7 to 14 and generally increased with decreasing concentration or increasing temperature. This is consistent with the view that the motion is becoming more isotropic with decreasing concentrations or increasing temperatures. As can be seen τ_0 is not always exponential in $1/T$. At higher concentrations there is a maximum with respect to $1/T$ which clearly mimics the T_1 behavior. Even in the most dilute solutions there is a slight nonexponential behavior. The apparent energies of activation calculated for τ_0, except for the most concentrated solutions, are given in Table III along with the values from the other models. It should be noted that the correlation times calculated for the most dilute solution are greater than some of the more concentrated ones.

The results from the VJGM model[4] are shown in Figure 4 for both parameters T_d and T_0. For the three-bond jump parameter T_d (Figure 4B), an Arrhenius-type behavior is found for concentrations less than 70 wt %. Above this concentration the nonlinear behavior is pronounced, with

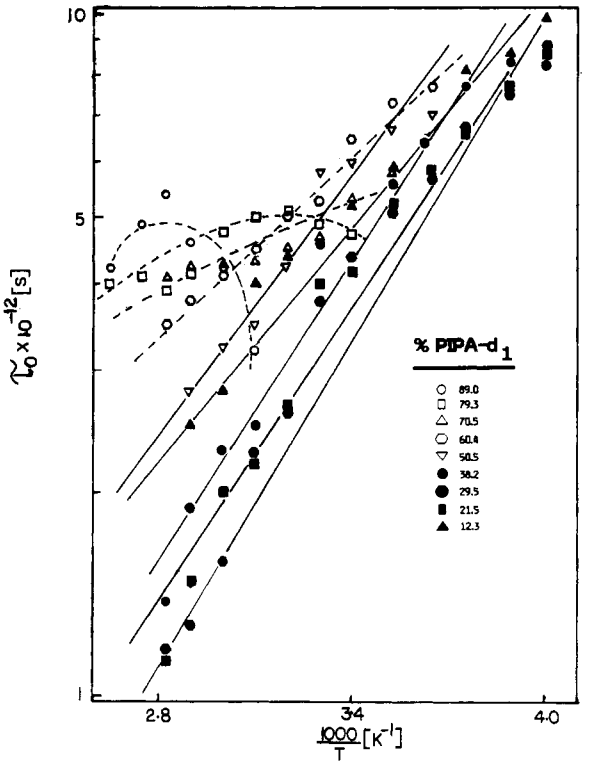

Figure 3. Calculated values of τ_0 from the log χ^2 model as a function of temperature and concentration. The lines are drawn to aid the eye.

maxima in T_d corresponding to the T_1 minima (Figure 2A). For dilute solution the energies of activation (Table III) are roughly independent of concentration and equal to 4–5 kcal/mol. In contrast, the behavior of T_0 with temperature suggests an Arrhenius-type behavior only at the highest concentrations and shows curvature for the lower concentrations. Energies of activation calculated for the more concentrated solutions ranged from 24 to 12 kcal/mol and monotonically decreased with decreasing concentration. The correlation times for T_0 are about 5 orders of magnitude lower than those for T_d. There is also a striking qualitative difference between the T_0 curves for concentrations of less than 40 wt % and greater than 40 wt %.

The results from the BY model are shown in Figure 5B (for ω_B) and Figure 5A (for ω_A). The low-frequency cutoff term ω_B is very similar to T_d from the VJGM model. The energies of activation from the BY model are also similar

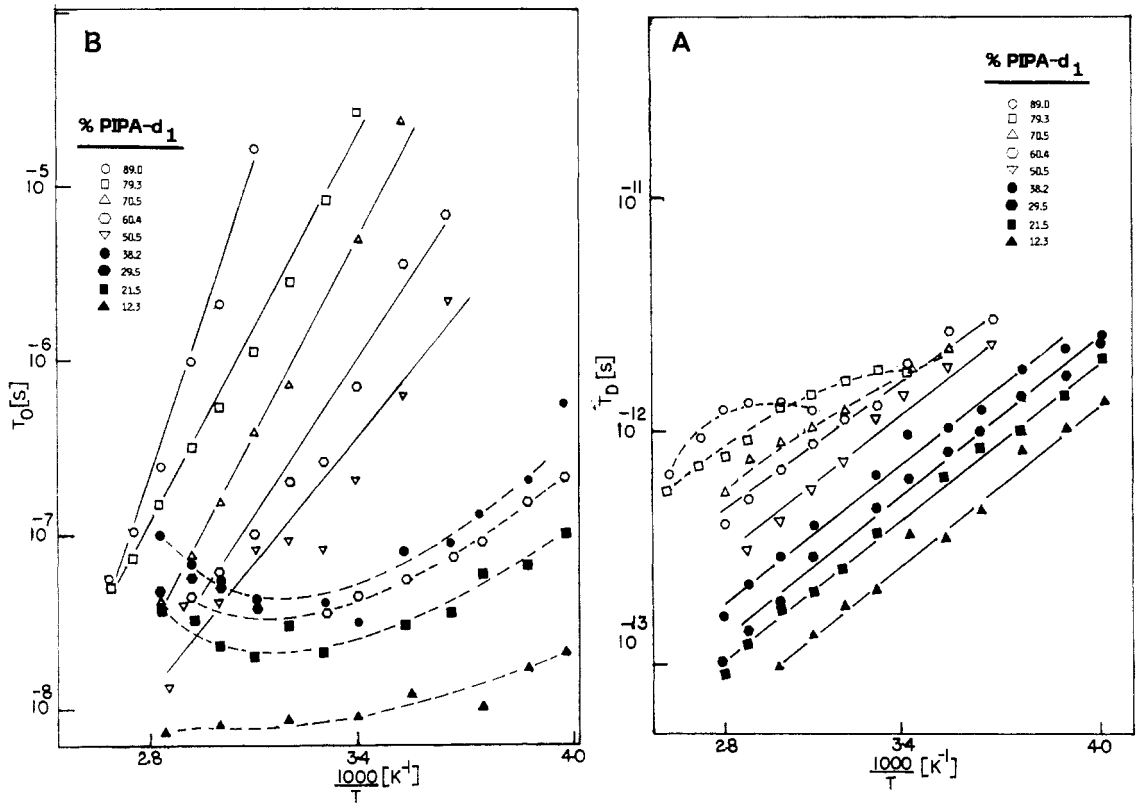

Figure 4. Calculated values of (A) T_0 and (B) T_d from the VJGM model as a function of temperature and concentration. The lines are drawn to aid the eye.

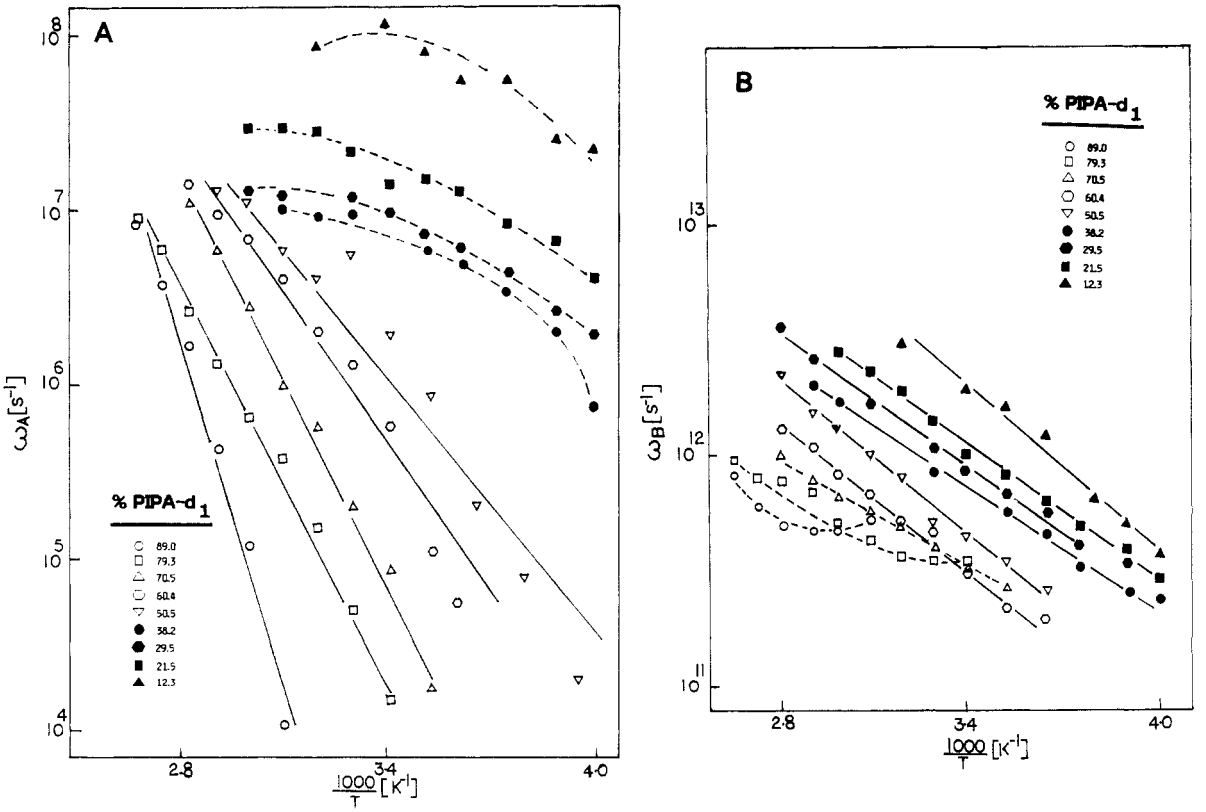

Figure 5. Calculated values of (A) ω_A and (B) ω_B from the BY model as a function of temperature and concentration. The lines are drawn to aid the eye.

to those from the VJGM model (Table III) for the fast-motional parameter. In addition, the concentrations which show curved behavior with $1/T$ are fairly similar for all three models. The results for the long-wavelength cut-off, ω_A (Figure 5A), are also similar to T_0 in the VJGM model. Both energies of activation and demarcation between 40 and 50 wt % are obvious. Values for ω_B are about 5 orders of magnitude faster than ω_A.

Finally, the results for the SY model are not explicitly shown because of their similarity to the BY results. The results from BY and SY are almost superimposable with $\delta \approx \omega_B$ and $\beta \approx \omega_A$. Slight differences do, however, result

in slightly different energies of activation which are given in Table III. Similar results would also be found by using the Jones and Stockmayer model.[16] The VJGM model is preferable in this case because the correlation lengths of the motions are long enough to make application of the Jones and Stockmayer model cumbersome.

Discussion

The data presented in the previous section represent an extensive set which can serve as a significant test for any motional model. In this study, all of the models previously mentioned can mimic the experimental data, but the results suggest that none of the models are totally applicable over the wide range of conditions employed here. However, it is still possible to use these models not only for comparison but also to yield physical insight into the polymer reorientation in these systems.

It is clear that the VJGM, BY, and SY models each have two parameters which can be associated with short-range and long-range (or alternatively fast and slow) motions. To an extent, τ_0 and P can be thought of in a similar way, although the formulation of the model is different. The values of the fast-motion parameters are dominated by T_1 and the slow-motion parameters by T_2. The curves for T_d, ω_B, and β are controlled mainly by T_1 as evidenced by marked curvature and extrema which correspond directly to the T_1 data. The log χ^2 distribution also has a similar relationship to T_1 as shown in the average correlation time curve. In the case of log χ^2, the width parameter is more sensitive to T_2 than T_1. However, it should be noted that the log χ^2 model does not seem to fit in a realistic way even for the most dilute solution data. The failure of the log χ^2 model in the dilute solution suggests that this model is probably not a realistic one for polymer motion. The fact that this was not observed in previous studies was due to the very limited data sets used.[3,25]

In dilute solution, the energies of activation are similar for the fast-motion parameters of all the models, with those for log χ^2 being slightly smaller than those from the other models. The smaller energies of activation probably result from the dominance of the fast correlation times in the log χ^2 distribution. Since the distribution rises very rapidly on the fast correlation time side, the fast correlation times tend to dominate τ_0.

For the other models (Table III) the energies of activation of 4–7 kcal/mol are very much in accord with previous studies. Similar values have been found for other polymer solutions reviewed by Heatley.[2] More recent results for poly(1-butene) (0.2 g/cm^3) in *o*-dichlorobenzene–deuteriobenzene (5.6 kcal/mol), polypropylene (4.1 kcal/mol),[18] and poly(methyl vinyl ketone) (15%) in dioxane (4.8 kcal/mol)[22] have similar E_a values. This is also in the range of the activation energy found for the aliphatic reorientation in solid poly(butylene terephthalate) (5.8 kcal/mol).[23] PBT has the smallest unit (butyl) which can undergo a variety of proposed three-bond motions even though there is some debate about the exact nature of these.[24] It is quite remarkable that so many systems have similar behavior with temperature changes in semidilute solution. This is especially interesting considering the different side chains which are encountered and the different motional models used. In our case, the insensitivity of the energies of activation to concentration is understandable if the fast, short-range bond motions do not require much free volume to occur and thus are not very sensitive to changes in concentration.

In more concentrated solutions the results for the fast-motion parameter are not monotonic functions of temperature. When the T_1 value approaches a minimum it is also mimicked in the fast-motion parameter. Similar behavior has also been noted using carbon-13 NMR in poly(butyl methacrylate) solutions.[25] We recognize that this is an obvious breakdown of all of the models used.

The slow-motion parameters have much higher energies of activation in concentrated solutions and are concentration dependent. As expected, the E_a decreases with decreasing concentration. This trend is most obvious for the VJGM and BY models. The higher energies of activation and slower motions are indicative of motions involving several subunits. At lower concentrations the slow-motional parameters have a more complicated temperature dependence. First noted[2] for the VJGM model, this problem is most likely due to the many different motions possible in dilute solutions which can contribute, each in their own way, to the temperature dependence.

It is surprising that the BY and SY models are almost identical in results despite their different formulation. This is disappointing considering that the SY model included a damping term which one might have thought would be very important in concentrated solution. The fact that similar results from both models are found is consistent with the current study and also the previous work of SY.[7] However, in contrast to their studies, we do not find any significant differences between the use of the VJGM, BY, or SY model. We feel that all three models yield the same information. It is interesting to compare our results with those of Heatley and Cox[26] as interpreted by Skolnick and Yaris.[7] Their data consisted of proton T_1 and NOE data. The curvature effects seen in the slow-motion parameter at low concentrations are evident even in their very limited data set. Consequently, it is not meaningful to interpret those data in terms of energies of activation. We therefore believe that their objections to the VJGM model, mostly based on energies of activation, are invalid. On the basis of this fact, neither our data nor theirs can make any definitive claims for a "best model".

In semidilute solution, the motion, as perceived from any of the models, is fast enough for both T_1 and T_2 to be dominated by fast motions. However, in concentrated solutions T_2 is dominated by much slower motions than those that determine T_1 because of the zero-frequency term in eq 2. This results in large differences in T_1 and T_2 for concentrated solutions. In previous proton NMR studies, proton dipolar coupling was suggested to be the dominant reason for the inequality of the relaxation times.[27] Unlike the proton case, the deuteron line widths and relaxation times in this study are not affected by low-speed sample rotation. This suggests that neither residual dipolar nor quadrupolar coupling is important when compared to the normal T_2 quadrupolar relaxation process. Therefore, we submit that the difference in T_1 and T_2 in this case is due to the nature of the motion itself (i.e., the reorientation of the C–D bond vector and not residual coupling as claimed for the proton case[27,28]).

Since T_2 becomes dominated by slower motions as the concentration is increased, it may serve as a means for estimating the rough division between semidilute and concentrated solutions. Shown in Figure 6 are the plots of the T_2 data between 10 and 50 °C as a function of the mole ratio of solvent to monomer units. As can be seen, the data for any temperature consist of two linear regions described previously as the concentrated and transition regions.[28]

The intersection of the two lines for each temperature in Figure 6 can be used to estimate a critical mole ratio, γ_c, and hence critical concentration, C_c. As expected, the critical concentration increases with increasing tempera-

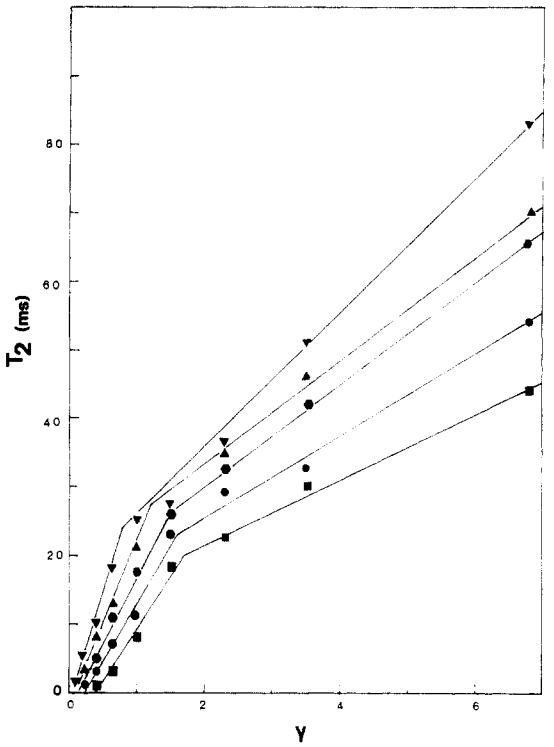

Figure 6. Deuterium spin–spin relaxation times (T_2) vs. γ, the mole ratio of solvent to monomer units, as a function of temperature: (▼) 50, (▲) 40, (●) 30, (●) 20, and (■) 10 °C.

Table IV
Comparison of the Critical Concentration (from Semidilute to Concentrated Regimes) and Intrinsic Viscosity of PIPA-*d*-$CHCl_3$ as a Function of Temperature

T, °C	$[\eta]$, mL/g	γ_c	C_c	$[\eta]C_c$
10	57	1.68	0.473	26.9
20	55	1.56	0.493	27.1
30	54	1.53	0.498	26.8
40	49	1.23	0.557	27.2
50	48	0.80	0.675	32.3

ture. The product of C_c and the intrinsic viscosity $[\eta]$ is listed in Table IV as a function of temperature. The product of these two is constant over the range studied (the 50 °C data show poor linear correlation in the semidilute region and may be discounted here). This suggests that for the PIPA–$CHCl_3$ system the transition to a strongly entangled regime is at about 30 times the concentration where $C_c[\eta] = 1$.

Previously, proton NMR studies have yielded results on the transition between dilute and semidilute solutions of polyisobutylene in carbon disulfide.[27,28] These results suggest that $C_c[\eta] = 10$ or 6 (depending on the molecular weight of the polymer). With this in mind, a value of 27 seems reasonable. Previous studies have not been easily able to probe this semidilute to concentrated solution transition. Proton NMR resonances often overlap in the concentrated region and so quantitative information is difficult to obtain.

The large differences between T_1's and T_2's in concentrated solutions are due to the different motions which dominate each. Hence a single theory does not appear to describe both simultaneously. Since T_2's are dominated by slow motions which involve many monomer units in the concentrated region, a free volume approach[29-31] may be applicable. In this case the superposition of both temperature and composition may be characterized by a shift factor

$$a(T,v_1) = (T_{2,0}/T_2) \tag{8}$$

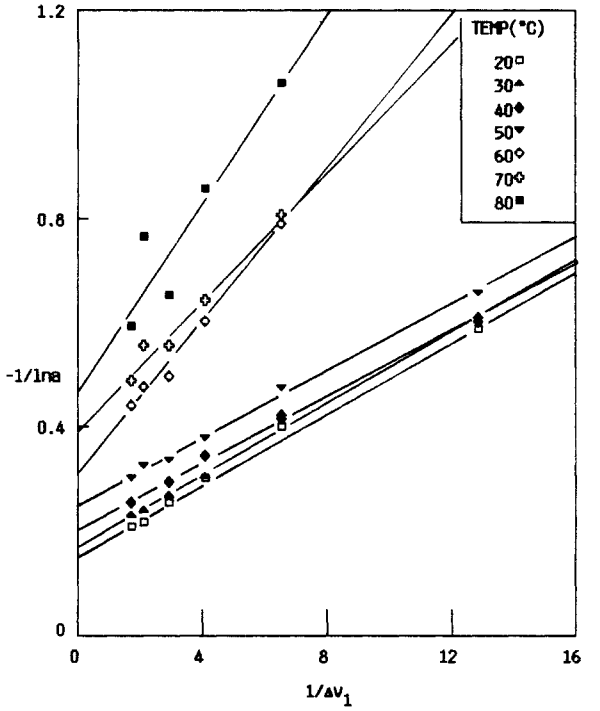

Figure 7. Shift factor for the T_2 data vs. $\Delta\delta_1$ as a function of temperature, using the data for 89 wt % PIPA sample as a reference.

where v_1 is the volume fraction of solvent and the zero subscript refers to an arbitary reference state. We note that the reference state is written in the numerator because the relaxation times vary inversely with the local friction coefficient upon which $a(T,v_1)$ is usually based.[29] Normally the shift factor dependence on the fractional free volume is given by

$$\ln a(T,v_1) = B[(1/f) - (1/f_0)] \tag{9}$$

where B is a constant close to unity and f and f_0 are the fractional free volumes of the solutions at T and v_1, and T_0 and $v_{1,0}$ (reference), respectively.

The T_2 data presented can be examined by using this approach by varying either the concentration or temperature. At a fixed temperature, the free volume may be given by

$$f = f_0 + \beta'(v_1 - v_{1,0}) \tag{10}$$

where β' can be related to the fractional free volumes of the pure components.[29] For the simple case where f is the volume fraction average of the free volumes of pure components, $\beta' = f_1^0 - f_2^0$, where the superscripts refer to the pure components. Substitution of eq 10 into eq 9 yields

$$-1/\ln a = f_0/B + f_0^2/B\beta'(v_1 - v_{1,0}) \tag{11}$$

The shift factors for the T_2 data are shown as a function of v_1 in Figure 7 for samples of 30 wt % or greater. Here the 89 wt % sample is used as a reference. The data show the linear dependence as expected from the theory and suggest the correctness of its application. The value of the intercept is seen to increase with increasing temperature and yields values shown in Table V. These values seem reasonable when compared to those of other systems for data obtained both from NMR[31] and from other techniques.[29] The slopes of the lines in Figure 7 are constant below 60 °C but increase by about a factor of 2 at 60 °C and are constant above 60 °C. This effect is seen in the calculated values of β'/B shown in Table V. At 60 °C there is a discontinuous jump in β'/B vs. temperature. This

Table V
Free Volume Parameters for Composition Superposition Using 89 wt % as Reference (Figure 7)

T, °C	f^0/B	β'/B
20	0.15	0.657
30	0.16	0.735
40	0.20	1.340
50	0.25	1.900
60	0.29	1.190
70	0.38	2.340
80	0.47	2.500

Table VI
Free Volume Parameters for Temperature Superposition Using the 20 °C Data as Reference (Figure 8)

wt % PIPA	f_0/B	B/α_f
89.0	0.091	1150
79.3	0.111	1250
70.5	0.149	731
60.4	0.118	1770
50.5	0.166	1110

temperature is very close to the normal boiling point of pure chloroform and so it may be tempting to suggest that the T_2 measurements are sensitive to this phenomenon. However, because calculation of β' involves multiplication of the intercept squared there may be considerable error in the calculated β' values.

The variation of free volume with temperture is often given by

$$f = f_0 + \alpha_f(T - T_0) \tag{12}$$

where α_f is the free volume thermal expansion coefficient. It is a composite of the expansion coefficients of the pure materials. Substitution of eq 12 into eq 8 yields

$$-1/\ln a = f_0/B + f_0^2/B\alpha_f(T - T_0) \tag{13}$$

The plot corresponding to our T_2 data and eq 13 is shown in Figure 8. In this case, we have examined the data as a function of composition using the 20 °C values as references. Again the data show linear behavior and the values of f_0/B and $\alpha f/B$ are shown in Table VI. The intercepts are again reasonable and generally increase with increasing concentration. The α_f parameters from the slope are shown to be more or less constant over the range studied. The 60 wt % data show a α_f value which is low, but this is most probably due to the very low value of the intercept for that sample.

The above discussion suggests that a free volume approach can describe the data. However, because the dependence of free volume on composition and temperature for this system is not known, independent comparisons have not been made. Work is presently being done in this laboratory using other techniques so that more than a semiquantitative approach can be taken for this system.

Conclusions

We have shown that the a combination of deuterium NMR T_1 and T_2 data is an effective probe of polymer segmental motion in the dilute and semidilute regions. In concentrated solutions, the T_2 data can give information on the longer time scale motion, which can be interpreted by using a free volume approach. The advantages of selective labeling with deuterium provide a means by which one can probe dynamics in both dilute and concentrated polymer solutions with excellent sensitivity and resolution. These techniques applied to poly(isopropyl acrylate-d) represent a very extensive probe of backbone motion.

In this study it was found that the log χ^2, VJGM, BY, and SY models could all mimic the data but it is clear that

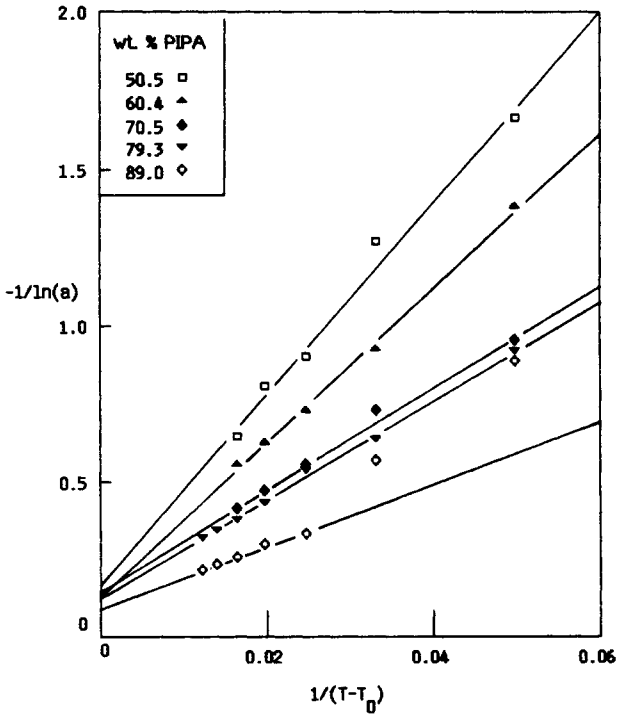

Figure 8. Shift factor for the T_2 data vs. $1/(T - T_0)$ as a function of concentration. T_0 is the reference temperature and equals 20 °C.

none of the models could be used successfully over the entire temperature–concentration range. It was found that all of the models essentially contain two parameters which were dominated by fast and slow motions. Thus, the fast- and slow-motional parameters were very closely coupled to the behavior of T_1 and T_2, respectively. Of the models tested, three yielded approximately the same view of the backbone dynamics (VJGM, BY, and SY) and therefore all are believed to be equally valid though none are successful over the entire concentration range. The log χ^2 model, however, probably underestimates the energies of activation and does not have physically realistic behavior for data from very dilute or concentrated solutions.

The results for poly(isopropyl acrylate-d) indicate that the fast motion involving a few bonds has an activation energy of about 5–7 kcal/mol for semidilute solutions. This activation energy is roughly independent of concentration and in agreement with results from other systems. The slow-motion parameter has a concentration-dependent energy of activation which is much higher than that for the fast motion. This is in agreement with the claim that it represents longer range segmental motions. The failure of the SY model was apparent even though its formulation made it very attractive for use in concentrated solution studies. The T_2 values were also shown to be useful to distinguish between semidilute and concentrated solutions. The division between these occurs at a concentration C_c, which as a function of temperature obeys $30 \approx [\eta]C_c$. Thus the T_2 values are very sensitive to chain overlap.

Finally, in concentrated solutions it was found that a free volume approach could be used to describe the T_2 behavior as a function of both temperature and composition. Plots of the shift factor $a(T,v_1)$ were linear with either $(T - T_0)^{-1}$ or $(v_1 - v_{1,0})^{-1}$, suggesting the correctness of this approach. The intercepts from both types of plots are consistent with fractional free volume that increases with increases in solvent concentration or temperature. They are also consistent with results from other systems which have similar dependences on free volume. The behavior of the parameters α_f and β' are more complicated

because the exact dependence of the free volume as a function of temperature and composition is not known. However, there does seem to be a change in slope, and hence β', in the range of the boiling point of chloroform.

Acknowledgment. The financial support of the donors of the Petroleum Research Fund, administered by the American Chemical Society, the Research Corp., the Drexel University Graduate School, and the Drexel University Computer Center is gratefully acknowledged. We also wish to thank the reviewers for helpful suggestions.

References and Notes

(1) Bailey, R. T.; North, A. M.; Pethrick, R. A. "Molecular Motion in High Polymers"; Clarendon Press: Oxford, 1981.
(2) Heatley, F. *Prog. NMR Spectrosc.* **1979**, *13*, 47.
(3) Schaefer, J. *Macromolecules* **1973**, *6*, 882.
(4) Valeur, B.; Jarry, J. P.; Geny, F.; Monnerie, L. *J. Polym. Sci., Polym. Phys. Ed.* **1975**, *13*, 667, 675, 2251.
(5) Bendler, J. T.; Yaris, R. *Macromolecules* **1978**, *11*, 650.
(6) Skolnick, J.; Yaris, R. *Macromolecules* **1982**, *15*, 1041.
(7) Skolnick, J.; Yaris, R. *Macromolecules* **1982**, *15*, 1046.
(8) Skolnick, J.; Yaris, R. *Macromolecules* **1983**, *16*, 266.
(9) For correction to ref 6, see: Yamakawa, H. *Macromolecules* **1983**, *16*, 491.
(10) Leitch, L. C. *Can. J. Chem.* **1957**, *35*, 345.
(11) Cockburn, W. F.; Hubley, C. E. *Appl. Spectrosc.* **1957**, *4*, 188.
(12) Brandrup, J.; Immergut, E. H., Eds. "Polymer Handbook"; Wiley: New York, 1975.
(13) Matsuzaki, K.; Kanai, T.; Kawamura, T.; Matsumoto, S. *J. Polym. Sci., Polym. Phys. Ed.* **1973**, *11*, 961.
(14) Farrar, T. C.; Becker, E. D. "Pulse and Fourier Transform NMR"; Academic Press: New York, 1971.
(15) Abragam, A. "Principles of Nuclear Magnetism"; Clarendon Press: Oxford, 1962.
(16) Jones, A. A.; Stockmayer, W. H. *J. Polym. Sci., Polym. Phys. Ed.* **1977**, *15*, 847.
(17) Lyerla, J. R.; Horikawa, T. T.; Johnson, D. E. *J. Am. Chem. Soc.* **1977**, *99*, 2463.
(18) Asakura, T.; Doi, Y. *Macromolecules* **1983**, *16*, 786.
(19) Inoue, Y.; Nishioka, A.; Chujo, R. *J. Polym. Sci., Polym. Phys. Ed.* **1973**, *11*, 2237.
(20) Grandjean, J.; Sillescu, H.; Willenverg, B. *Makromol. Chem.* **1977**, *178*, 145.
(21) Adriansens, G. J.; Bjorkstan, J. L. *J. Chem. Phys.* **1972**, *56*, 1123.
(22) Mashimo, S.; Winsor, P.; Cole, R.; Matso, K.; Stockmayer, W. H. *Macromolecules* **1983**, *16*, 965.
(23) Jelinski, L. W.; Dumais, J. J.; Engel, A. K. *Macromolecules* **1983**, *16*, 492.
(24) Skolnick, J.; Helfand, E. *J. Chem. Phys.* **1980**, *72*, 5489.
(25) Levy, G. C.; Axelson, D. E.; Schwartz, R.; Hochmann, J. *J. Am. Chem. Soc.* **1978**, *100*, 410.
(26) Heatley, F.; Cox, M. *Polymer* **1977**, *18*, 399.
(27) Cohen-Addad, J. P.; Guillermo, A.; Messa, J. P. *Polymer* **1979**, *20*, 536.
(28) Cohen-Addad, J. P. *J. Chem. Phys.* **1979**, *71*, 3689.
(29) Ferry, J. D. "Viscoelastic Properties of Polymers"; Wiley: New York, 1983.
(30) Turnbull, D.; Cohen, M. H. *J. Chem. Phys.* **1961**, *34*, 120.
(31) Cohen-Addad, J. P.; Faure, J. P. *J. Chem. Phys.* **1974**, *61*, 1571.
(32) We have also fit our data to the model of Hall and Helfand (*J. Chem. Phys.* **1982**, *77*, 3275) using the spectral density reported by Connolly et al. (*Macromolecules*, **1984**, *17*, 722). The results were deemed nonphysical and this was probably due to the different frequencies of motion associated with T_1 and T_2. The Hall–Helfand model is specifically derived for very short-range motions and apparently cannot accommodate the longer range motions to which the T_2 is sensitive.

A General Linear-Viscoelastic Theory for Nearly Monodisperse Flexible Linear Polymer Melts and Concentrated Solutions and Comparison of Theory and Experiment

Y.-H. Lin

Exxon Chemical Company, Plastics Technology Division, Baytown, Texas 77522.
Received March 13, 1984

ABSTRACT: Rheological properties are much related to the molecular dynamics in concentrated polymer systems. The reptational chain model of Doi and Edwards has successfully explained many characteristic features of viscoelasticity of flexible linear polymers. The Doi–Edwards theory predicts that the zero-shear viscosity scales with molecular weight, M, as $\eta_0 \propto M^3$ while the well-known experimental result is $\eta_0 \propto M^{3.4}$. This discrepancy is a fundamental pending problem associated with the molecular theory. We have theoretically identified four modes of polymer dynamics: the Rouse motion between two entanglement points, the chain slippage through entanglement links, the chain contour length fluctuation, and the chain reptational motion corrected for the chain length fluctuation effect. Including all these four dynamic modes, a general functional form for the stress relaxation modulus after a step shear deformation in the linear region has been derived. Extensive and consistent agreements between theory and experiment have been obtained. The theory allows the analysis of the entire linear viscoelastic spectrum and explains (a) the 3.4 power law of viscosity as a function of molecular weight, (b) the molecular weight dependence of steady-state compliance, (c) the transition point of viscosity, M_c, and (d) the transition point of the steady-state compliance M_c'. We have used the theory "literally" in analyzing experimental data. The consistency observed in the agreements of theory and experiment may allow for exact definition of several fundamental physical quantities in polymer dynamics and viscoelasticity.

I. Introduction

Linear viscoelasticity of polymers is a very important aspect of rheological study. On one hand it is closely related to the molecular structure (molecular weight (MW), molecular weight distribution (MWD), and long branches),[1] and on the other hand it determines the relaxation of polymer stress or orientation in processing.[2,3] Thus, it plays an essential role in linking polymer structure and processing. Despite its importance, a completely good understanding of its relation with molecular structure has been lacking even for the simplest cases such as flexible linear polymers of very narrow MWD.

In 1971, de Gennes[4] described the diffusion of a linear polymer molecule in a network system as reptation in a "tube". In 1978, Doe and Edwards[5-8] recognized the important relation of the reptational motion and the me-

0024-9297/84/2217-2846$01.50/0